Solar Energy Materials & Solar Cells 120 (2014) 94–101

Contents lists available at ScienceDirect

Solar Energy Materials & Solar Cells

journal homepage: www.elsevier.com/locate/solmat

Enhanced photocurrent generation by high molecular weight random copolymer consisting of benzothiadiazole and quinoxaline as donor materials

Doo Hun Kim, Ho Jun Song, Soo Won Heo, Kwan Wook Song, Doo Kyung Moon *

Department of Materials Chemistry and Engineering, Konkuk University, 1 Hwayang-dong, Gwangjin-gu, Seoul 143-701, Republic of Korea

ARTICLE INFO

Article history:
Received 24 April 2013
Received in revised form
16 August 2013
Accepted 19 August 2013
Available online 25 September 2013

Keywords:
Randomcopolymer
OPVs
Conjugated polymer
Benzothiadiazole
Quinoxaline

ABSTRACT

We synthesized organic photovoltaic materials that have high molecular weight and good solubility. A new random copolymer named poly[carbazole-co-dithienylbenzothiadiazole-co-dithienylquinoxaline] (PC-TBT-TQ) was polymerized through the Suzuki coupling reaction. PC-TBT-TQ was dissolved in a common organic solvent, and its M_n indicates a high molecular weight of 216.2 kg/mol. According to the result of thermal analysis, very high thermal stability was observed, with an approximately 5 wt% weight loss at 440 °C. The optical band gap of PC-TBT-TQ (1.89 eV) is slightly higher than that of PCDTBT (1.87 eV). The HOMO and LUMO levels of PC-TBT-TQ (HOMO level: 5.45 eV, LUMO level: 3.56 eV) are similar to those of PCDTBT (HOMO level: 5.45 eV, LUMO level: 3.58 eV). The OPV properties of the polymer were assessed by fabricating bulk-heterojunction polymer solar cells in the ITO/PEDOT:PSS/active-layer/BaF_2/Ba/Al structure. When PC-TBT-TQ and $PC_{71}BM$ were fabricated in a 1:4 ratio, the open-circuit voltage (V_{OC}), short-circuit current (J_{SC}), fill factor (FF) and power conversion efficiency (PCE) were 0.83 V, 9.5 mA/cm^2, 43.3% and 3.5%, respectively.

© 2013 Elsevier B.V. All rights reserved.

1. Introduction

For decades, semiconducting polymers have been studied in various fields, including organic light-emitting diodes (OLEDs) [1–3], organic photovoltaic cells (OPVs) [4–10] and organic thin-film transistors (OTFTs) [11,12]. In these applications, OPVs have been in the spotlight as a trending global technology due to their economic efficiency and ability to facilitate sustainable development without environmental destruction. Nevertheless, low power conversion efficiency (PCE) has been the greatest barrier to OPV applications [5].

To improve the PCE, the following ideal conditions should be met in a conjugated polymer: (1) low band gap with a broad light-absorption range, (2) crystal structure for good charge transport, (3) low HOMO energy level to obtain a high open-circuit voltage (V_{OC}) and (4) high molecular weight to improve the photocurrent.

Studies on the improvement of the photocurrent by creating polymers with high molecular weight have recently been reported [13,14]. The higher the molecular weight of a polymer is, the longer its conjugation length becomes. Therefore, more photons can be absorbed and thus higher photocurrent can be generated. In other words, it is necessary to introduce derivatives with good solubility when the molecular structure of a polymer is designed to have a high molecular weight.

Over the past few years, donor–acceptor (D–A)-type low-band-gap polymers have drawn great attention because their electronic properties can be easily modified through their unique bonding properties and their absorption range can be increased to capture long wavelengths of light. D–A polymers exhibit a wide range of molecular weights depending on the solubility of the acceptor.

The quinoxaline derivative, which contains electron-withdrawing nitrogen atoms, is highly electron-deficient and thus serves as an efficient electron acceptor; therefore, it easily forms intramolecular charge transfer (ICT) complexes with other donor components [15,16]. In addition, the quinoxaline derivative can have high solubility and be easily transformed structurally. Its electronic properties can also be modified by adding various substituents [17,18].

In this study, a polymer with a high molecular weight named poly[carbazole-co-dithienylbenzothiadiazole-co-dithienylquinoxaline] (PC-TBT-TQ) was polymerized by introducing quinoxaline (an acceptor unit with high solubility) and benzothiadiazole (an acceptor unit with high absorbance). To increase the solubility of the *n*-type polymer and stabilize excitons created by resonance effects in molecules, hexyloxybenzene was introduced into the quinoxaline unit [16]. In addition, the optical and electrochemical properties as a function of molecular weight were analyzed comparatively by polymerizing the well-known poly[carbazole-benzothiadiazole] (PCDTBT). The photovoltaic conversion efficiencies

* Corresponding author. Tel.: +82 2 450 3498; fax: +82 2 444 0765.
E-mail address: dkmoon@konkuk.ac.kr (D.K. Moon).

0927-0248/$ - see front matter © 2013 Elsevier B.V. All rights reserved.
http://dx.doi.org/10.1016/j.solmat.2013.08.021

of PCDTBT and PC-TBT-TQ were compared by fabricating a bulk-heterojunction device using $PC_{71}BM$ (3′H-cyclopropa[8,25][5,6]full-erene-C70-D5h(6)-3′-butanoic acid, 3′-phenyl-, methyl ester).

2. Experimental section

2.1. Instruments and characterization

Unless otherwise specified, all reactions were carried out under a nitrogen atmosphere. Solvents were dried using standard procedures. All column chromatography was performed using silica gel (230–400 mesh, Merck) as the stationary phase. ^{1}H–NMR spectra were measured on a Bruker ARX 400 spectrometer using solutions in $CDCl_3$, and chemical signatures were recorded in units of ppm with TMS as the internal standard. The elemental analyses were measured with an EA1112 using a CE Instrument. Electronic absorption spectra were measured in chloroform using an HP Agilent 8453 UV–vis spectrophotometer. Cyclic voltammetric curves were produced using a Zahner IM6eX electrochemical workstation with a 0.1 M acetonitrile (substituted with nitrogen for 20 min) solution containing tetrabutyl ammonium hexafluorophosphate (Bu_4NPF_6) as the electrolyte at a constant scan rate of 50 mV/s. ITO, a Pt wire and silver/silver chloride [Ag in 0.1 M KCl] were used as the working, counter and reference electrodes, respectively. The electrochemical potential was calibrated against Fc/Fc^+. The HOMO levels of the polymers were determined using the oxidation onset value. Onset potentials are the potential values obtained from the intersection of the two tangents drawn at the rising current and the baseline changing current of CV curves. TGA measurements were performed on a NETZSCH TG 209 F3 thermogravimetric analyzer. All GPC analyses were conducted using THF as the eluant and polystyrene standard as the reference. X-ray diffraction (XRD) patterns were obtained using a SmartLab diffractometer operated at 3 kW (40 kV 30 mA, Cu target, wavelength: 1.541871 ang), Rigaku, Japan. Topographic images of the active layers were obtained through atomic force microscopy (AFM) in tapping mode under ambient conditions using an XE-100 instrument.

2.2. Fabrication and characterization of polymer solar cells

All of the bulk-heterojunction PV cells were prepared using the following device fabrication procedure. Glass/indium tin oxide (ITO) substrates [Sanyo, Japan (10 Ω/γ)] were sequentially patterned lithographically, cleaned with detergent and ultrasonicated in deionized water, acetone and isopropyl alcohol. The substrates were then dried on a hot plate at 120 °C for 10 min and treated with oxygen plasma for 10 min to improve the contact angle immediately before the film-coating process. Poly(3,4-ethylenedioxythiophene):poly(styrene-sulfonate) (PEDOT:PSS, Baytron P 4083 Bayer AG) was passed through a 0.45-μm filter before being deposited onto ITO at a thickness of *ca.* 32 nm by spin-coating at 4000 rpm in air; it was then dried at 120 °C for 20 min inside a glove box. Composite solutions of the polymers and PCBM were prepared using 1,2-dichlorobenzene (DCB). The concentration was controlled adequately over a 0.5 wt% range, and the solutions were then filtered through a 0.45-μm PTFE filter and then spin-coated (500–2000 rpm, 30 s) on top of the PEDOT:PSS layer. Device fabrication was completed by depositing thin layers of BaF_2 (1 nm), Ba (2 nm) and Al (200 nm) at pressures below 10^{-6} Torr. The active area of the device was 4.0 mm^2. Finally, the cells were encapsulated using UV-curing glue (Nagase, Japan). In this study, all of the devices were fabricated with the following structure: ITO glass/PEDOT:PSS/polymer:PCBM/BaF_2/Ba/Al/encapsulation glass.

The illumination intensity was calibrated using a standard Si photodiode detector that was equipped with a KG-5 filter. The output photocurrent was adjusted to match the photocurrent of the Si reference cell to obtain a power density of 100 mW/cm^2. After the encapsulation, all of the devices were operated under ambient atmosphere at 25 °C. The current–voltage (*I–V*) curves of the photovoltaic devices were measured using a computer-controlled Keithley 2400 source measurement unit (SMU) that was equipped with a Peccell solar simulator under AM 1.5 G (100 mW/cm^2) illumination. The thicknesses of the thin films were measured using a KLA Tencor Alpha-step 500 surface profilometer with an accuracy of 1 nm.

Hole-only devices were fabricated with a diode configuration of ITO (170 nm)/PEDOT:PSS (40 nm)/polymer:$PC_{71}BM$ (50 nm)/MoO_3 (30 nm)/Al (100 nm). The hole mobilities of the active layers were calculated from the SCLC using the *J–V* curves of the hole only devices in the dark as follows:

$$J=\frac{9}{8}\varepsilon_r\varepsilon_0\mu_{h(e)}\frac{V^2}{L^3}\exp\left(0.89\sqrt{\frac{V}{E_0L}}\right)$$

where ε_0 is the permittivity of free space (8.85×10^{-14} C/Vcm); ε_r is the dielectric constant (assumed to be 3, which is a typical value for conjugated polymers) of the polymer; $\mu_{h(e)}$ is the zero-field mobility of holes (electrons); L is the film thickness; and $V=V_{appl}-(V_r+V_{bi})$, where V_{appl} is the voltage applied to the device, V_r is the voltage drop due to series resistance across the electrodes and V_{bi} is the built-in voltage.

2.3. Materials

All reagents were purchased from Aldrich, Acros or TCI. All chemicals were used without further purification. The following compounds were synthesized following modified literature procedures: 4,7-bis(5-bromothiophen-2-yl)benzo[c][1,2,5]thiadiazole (M2) [17], 5,8-bis(5-bromothiophen-2-yl)-2,3-bis(4-(hexyloxy)phenyl)quinoxaline (M3) [16].

2.3.1. Poly[carbazole-co-dithienylbenzothiadiazole-co-dithienylquinoxaline] (PC-TBT-TQ)

9-(Heptadecan-9-yl)-2,7-bis(4,4,5,5-tetramethyl-1,3,2-dioxaborolan-2-yl)-9H-carbazole (M1) (0.36 g, 0.55 mmol), 4,7-bis(5-bromo thiophen-2-yl)benzo[c][1,2,5]thiadiazole(M2)(0.115 g,0.25 mmol), 5, 8-bis(5-bromothiophen-2-yl)-2,3-bis(4-(hexyloxy)phenyl)quinoxaline(M3)(0.201 g,0.25 mmol)Pd(PPh_3)$_4$(0)(0.017 g, 0.015 mmol) and aliquat336 were placed in a Schlenk tube, purged by performing three nitrogen/vacuum cycles and, under a nitrogen atmosphere, added with 2 M degassed aqueous K_2CO_3 (10 mL) and dry toluene (20 mL). The mixture was heated to 90 °C and stirred in the dark for 48 h. Following polymerization, the polymer was end-capped with bromothiophene. After quenching the reaction, the entire mixture was poured into methanol. The precipitate was filtered off and purified by Soxhlet extraction in the following order: methanol, acetone and chloroform. The polymer was recovered from the chloroform fraction and precipitated in methanol. The final product was obtained after drying in vacuum. Dark purple solid. (0.42 g, 41%) Anal. Calcd for $C_{114}H_{134}N_6O_2S_5$:C, 76.89; H, 7.59; N, 4.72; S, 9.00; O, 1.8. Found: C, 75.26; H, 7.40; N, 4.59; S, 8.85; O, 2.8.

3. Results and discussion

3.1. Material synthesis

As shown in Scheme 1, the polymer was polymerized through the Suzuki coupling reaction with molar ratios of 50%, 25% and 25%

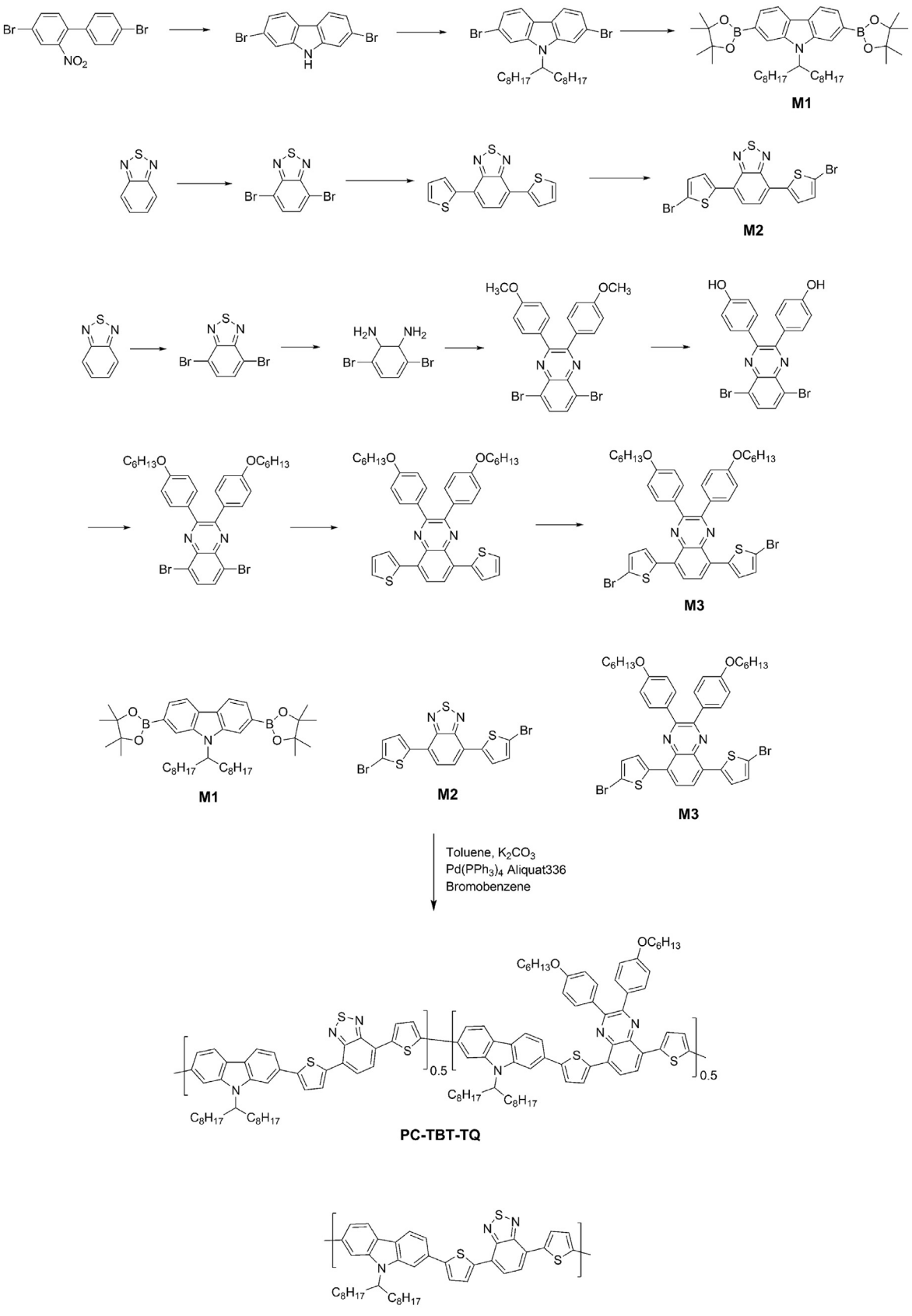

Scheme 1. Scheme of monomer synthesis and polymerization.

for the monomers M1, M2 and M3, respectively, and the yield was 47%. PCDTBT showed a particularly interesting PCE in excess of 6% in a BHJ cell. However, there is the drawback that the solubility decreases as the molecular weight increases. In this regard, we focused our attention on the well-known quinoxaline derivative, which is an acceptor unit with high solubility and benzothiadiazole derivative, which is one of the stronger electron-withdrawing moieties used widely in PSCs, due to a combination of its electron accepting properties. It was polymerized at 90 °C for 48 h using palladium (catalyst), 2 M potassium carbonate solution, aliquat 336 (surfactant) and toluene (solvent). Following polymerization, the polymer was end-capped with bromothiophene. The synthesized polymer was purified using a Soxhlet extractor with methanol, acetone and chloroform. The polymer was recovered from the chloroform fraction and precipitated. All polymers were dissolved in common organic solvents such as THF, chloroform, chlorobenzene and o-dichlorobenzene. By spin-coating, a uniform and violet semi-transparent film was formed.

Fig. 1 shows the ^{1}H NMR spectra of the polymer samples. As shown in Fig. 1, the aromatic peaks were observed at 7.0–8.0 ppm, whereas the proton peaks, which originated from aliphatic peaks, were observed at 0.8–3.0 ppm. The peak at 4.0 ppm is the proton peak of O–CH_2 in M3, whereas the peak at 5.0 ppm is the proton peak of N–CH in M1. Although it is a random copolymer, when the intensity of the protons was compared, the contents of M1, M2 and M3 were determined to be close to 50%, 25% and 25%, respectively. Table 1 shows the results of the analysis of the molecular weight of PC-TBT-TQ. As shown in Table 1, GPC was performed using polystyrene as a standard; the number-average molecular weight (M_n) was 216.2 kg/mol, and the polydispersity index (PDI) was 1.47 with a very narrow distribution. The degree of polymerization of PC-TBT-TQ was 5–6 times higher than that of other OPV polymers. The M_n was approximately 11 times higher than that of PCDTBT (18.4 kg/mol) [19]. It appears that the degree of polymerization was high because the addition of M3 increased the solubility of the polymer, which exhibited a relatively good backbone structure [16]. Because the M_n of PC-TBT-TQ (216.2 kg/mol) was greater than that of PCDTBT (18.4 kg/mol), a higher photocurrent is expected for PC-TBT-TQ-based devices than for PCDTBT-based devices [13]. According to elemental analysis, the theoretical data (C:76.89, H:7.59, N:4.72, S:9.00, O:1.8) are nearly identical to the experimental data (C:75.26, H:7.40, N:4.59, S:8.85, O:2.8). Therefore, it was confirmed that polymerization occurred close to the ratio before polymerization (M1:M2:M3 ratio of 50:25:25), which was also confirmed detected by ^{1}H NMR.

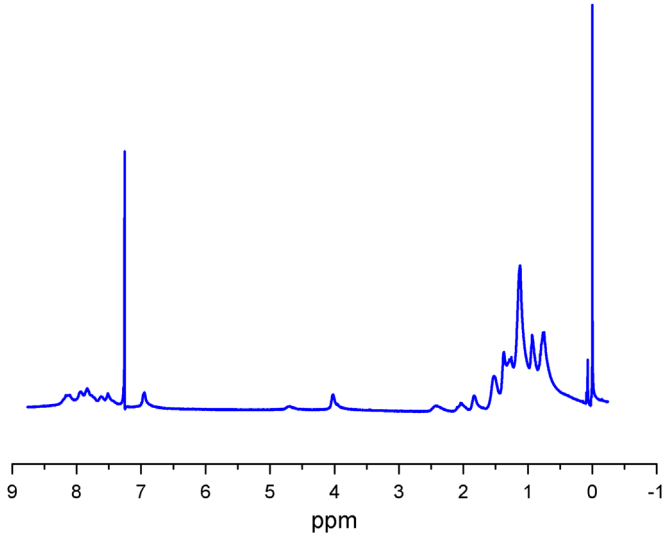

Fig. 1. ^{1}H–NMR spectrum of PC-TBT-TQ.

Table 1
Molecular weight and thermal properties of the polymers.

Polymer	M_n (kg/mol)	M_w (kg/mol)	PDI	T_d (°C)[a]
PC-TBT-TQ	216.2	317.6	1.47	449
PCDTBT	18.4	27.8	1.51	–

[a] Temperature resulting in 5% weight loss based on initial weight.

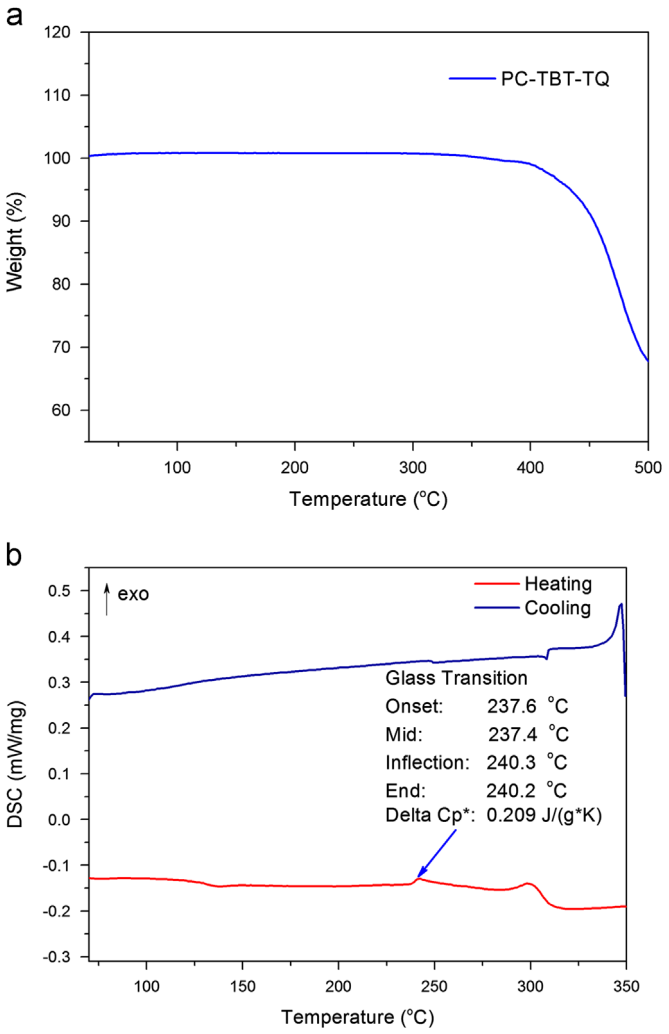

Fig. 2. (a) TGA and (b) DSC curves of polymers.

3.2. Thermal properties

Fig. 2(a) shows the TGA curve of PC-TBT-TQ. According to TGA, very high thermal stability was observed, with an approximately 5 wt% loss at 440 °C. Previous studies have demonstrated OPV polymers that undergo 5 wt% weight loss at 350–400 °C. In comparison, PC-TBT-TQ exhibited 40–90 °C higher thermal stability because it possessed an M_n value 3–4 times greater than that of other polymers [19]. In addition, the polymer can be applied in polymer solar cells, which require high thermal stability (300 °C or higher), and other opto-electronic devices [20].

Fig. 2(b) shows the DSC curve of PC-TBT-TQ. According to the DSC results, the glass transition temperature (T_g) was observed to occur at approximately 135 °C, and an endothermic transition (T_m) along with a transition enthalpy ($\triangle H$) of 0.209 J g^{-1} was observed

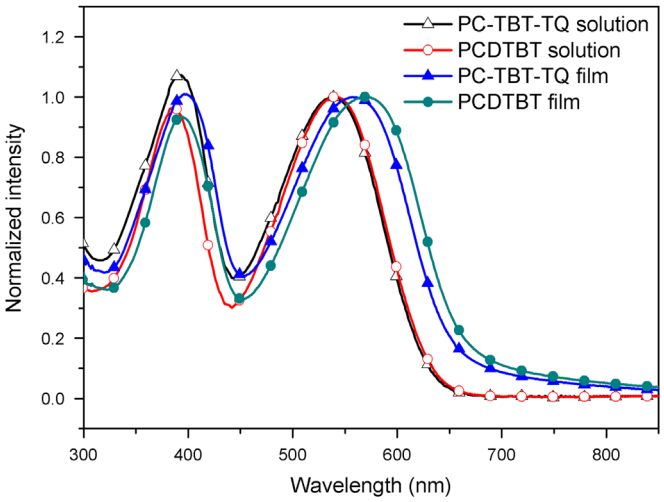

Fig. 3. Absorption spectra of PC-TBT-TQ in solution (10^{-6} M) and film (50 nm).

at 237 °C. Therefore, it was confirmed that a high amorphous fraction occurs in the film state. In addition, the transition enthalpy is greater than that of other polymers in terms of crystallinity [21].

3.3. Optical and electrochemical properties

Fig. 3 shows the UV–visible spectra obtained after forming a solution (10^{-6} M) and spin-coating a 50-nm thin film by dissolving PC-TBT-TQ o-dichlorobenzene (o-DCB). As shown in Fig. 3, the maximum absorption peaks (λ_{max}) of PC-TBT-TQ were observed at 392 nm and 540 nm in solution. The absorption band at 392 nm was attributed to the $\pi-\pi^*$ transition of the conjugated backbone, whereas the one at 540 nm was formed by ICT between donor and acceptor moieties [22]. In the case of the film, the maximum absorption peaks (λ_{max}) of PC-TBT-TQ were observed at 397 nm and 557 nm, which were red-shifted by 5–17 nm when compared to the solution spectrum because more planar conformations were observed during film formation [22]. A PCDTBT film band edge (662 nm) occurring at a longer wavelength than the PC-TBT-TQ film band edge (654 nm) was observed. The optical band gap energy of PC-TBT-TQ, which was calculated by considering the type of band edge, was 1.89 eV, slightly higher than that of PCDTBT (1.87 eV).

Fig. 4(a) shows the results obtained from cyclic voltammetry (CV) measurements. To verify the HOMO and LUMO levels of PC-TBT-TQ, cyclic voltammograms were measured, and the results are shown in Table 2 and Fig. 4(a). In PC-TBT-TQ, the HOMO and LUMO levels were 5.45 eV and 3.56 eV, respectively, which are similar to those of PCDTBT (HOMO level: 5.45 eV, LUMO level: 3.58 eV). Because the HOMO level is lower than that of P3HT (4.9 eV), relatively high air stability and a high open-circuit voltage (V_{OC}) are expected [23].

Fig. 4(b) shows the energy levels of ITO, PEDOT:PSS, PCDTBT, PC-TBT-TQ, $PC_{71}BM$ and Al in a band diagram. As shown in Fig. 4 (b), the LUMO level of PC-TBT-TQ (3.56 eV) is 0.34 eV lower than that of $PC_{71}BM$ (3.9 eV). The HOMO level of PC-TBT-TQ (5.45 eV) is 0.45 eV higher than that of PEDOT:PSS (5.0 eV).

3.4. Orientation analysis

To analyze the ordering structure of the polymers, X-ray diffraction of the thin films was performed, and the results are shown in Fig. 5. The out-of-plane peak, observed in all diffraction

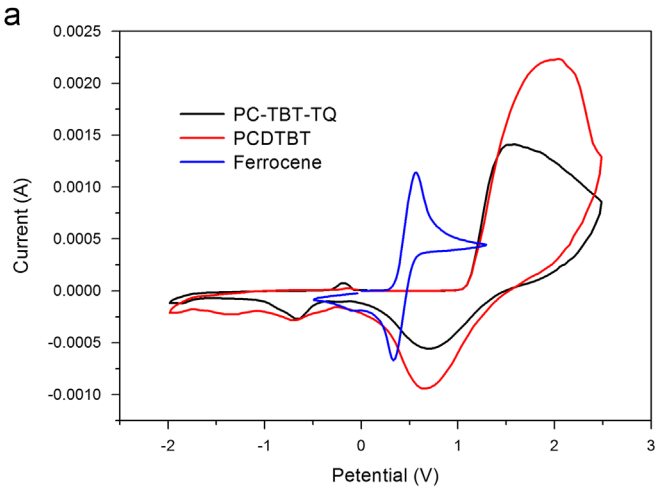

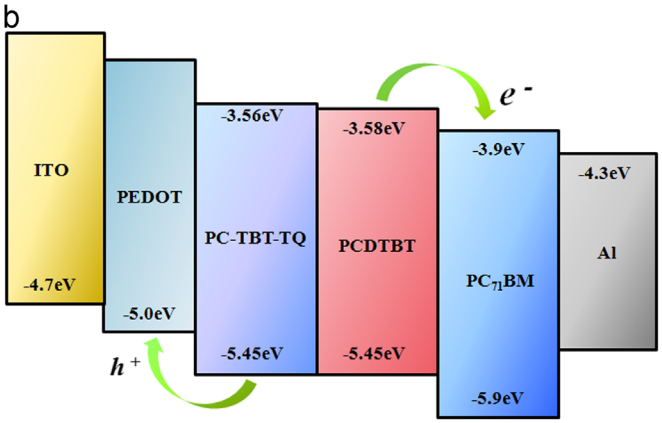

Fig. 4. (a) Cyclic voltammogram of PC-TBT-TQ (b) band diagram of polymers.

Table 2
Optical and electrochemical properties of the polymers.

Polymer	Absorption, λ_{max} (nm)		E_{ox}^{onset} (V)	E_{HOMO} (eV)[c]	E_{LUMO} (eV)[d]	E_{opt} (eV)[e]
	Solution[a]	Film[b]				
PC-TBT-TQ	392,540	397,557	1.14	−5.45	−3.56	1.89
PCDTBT	356,540	396,570	1.14	−5.45	−3.58	1.87

[a] Absorption spectrum in $CHCl_3$ solution (10^{-6} M).
[b] Spin-coated thin film (50 nm).
[c] Calculated from the oxidation onset potentials under the assumption that the absolute energy level of Fc/Fc+ was −4.8 eV below a vacuum.
[d] HOMO−E_{opt}.
[e] Estimated from the onset of UV–vis absorption data of the thin film.

patterns of highly ordered lamellar polymeric structures, did not occur.

In the out-of-plane direction of PC-TBT-TQ, the (1 0 0) crystal plane was observed at 4.1 °, which indicates the formation of an ordered lamellar structure. In addition, along the (0 1 0) crystal plane related to $\pi-\pi$ stacking, a broad diffraction peak was observed at 21.0°. Using the equation ($\lambda=2d\sin\theta$), the $\pi-\pi$ stacking distance (d_π) of PC-TBT-TQ was determined to be 4.2 Å [17,24]. With respect to the diffraction pattern of PCDTBT, the result for the (0 1 0) crystal plane is similar to that of PC-TBT-TQ. The $\pi-\pi$ stacking distance (d_π) was determined to be 4.2 Å. This result is similar to the $d\pi$ (4.0–4.4 Å) of benzene–thiophene aromatic system polymers that perform well as OPVs [25].

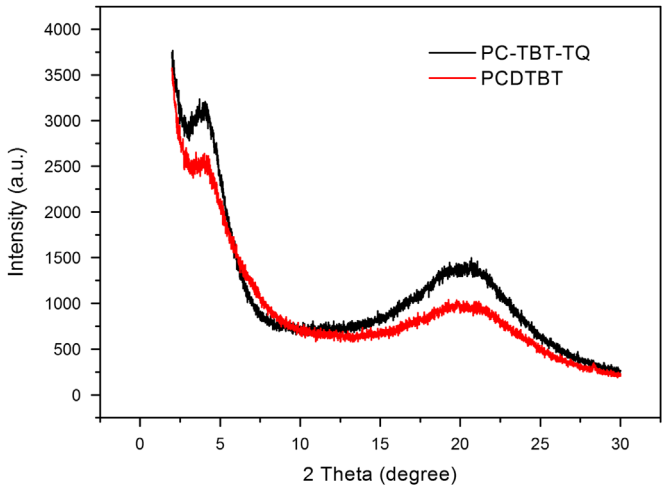

Fig. 5. Out-of-plane X-ray diffraction pattern in thermally treated thin films.

Interestingly, the (0 1 0) diffraction of PC-TBT-TQ corresponding to π–π stacking with a *d*-spacing of 4.2 Å was more prominent than that of PCDTBT. This result suggests that a large fraction of the PC-TBT-TQ backbones were oriented face-on relative to the substrate. In other words, the π-stacking direction was perpendicular to that of the substrate [26].

Therefore, PC-TBT-TQ is more effective than PCDTBT in terms of photo-current production and charge transport.

3.5. Photovoltaic characteristics

Fig. 6 and Table 3 show the measured properties of the OPV devices. The devices were fabricated in the following structure: ITO/PEDOT:PSS/active-layer/BaF_2/Ba/Al. In addition, an active layer with a thickness of 50–60 nm was created by spin-coating after being dissolved in o-dichlorobenzene at various polymer:$PC_{71}BM$ weight ratios (1:0.8, 1:1, 1:2, and 1:4).

As shown in Fig. 6(a) and Table 3, as the content of $PC_{71}BM$ was increased, the short-circuit current (J_{SC}) and power conversion efficiency (PCE) of PC-TBT-TQ improved because more photons could be absorbed. As the ratio of $PC_{71}BM$ increases, in other words, a hole percolation path that makes it possible to collect electric charge at the electrodes effectively is formed, and excited states are suppressed [27]. When PC-TBT-TQ and $PC_{71}BM$ were fabricated in a 1:4 ratio, the open-circuit voltage (V_{OC}), J_{SC}, fill factor (FF) and PCE were 0.83 V, 9.5 mA/cm^2, 43.3% and 3.5%, respectively. When PCDTBT and $PC_{71}BM$ were fabricated in a 1:4 ratio, the V_{oc}, J_{sc}, FF and PCE were 0.89 V, 7.8 mA/cm^2, 47.5% and 3.3%, respectively. The photocurrent of PC-TBT-TQ was higher than that of PCDTBT because the M_n of PC-TBT-TQ (216.2 kg/mol) was greater than that of PCDTBT (18.4 kg/mol) [13,14].

To verify the accuracy of the device measurements, the external quantum efficiency (EQE) was measured. The EQE curve shown in Fig. 6(b) is plotted as a function of $PC_{71}BM$ content. Because photons are mostly absorbed in the polymer phase, the EQE curve is correlated with the absorption spectra of a polymer [5]. As shown in Fig. 6(b), the EQE curve is similar to the UV–vis spectrum shown in Fig. 1. In the range of 400–600 nm, as the $P_{71}CBM$ ratio increased, the EQE increased from 50% to 60% because PCBM can absorb more photons [5]. For PC-TBT-TQ, the short-circuit current density obtained from the EQE versus $PC_{71}BM$ (1:4 ratio) curve was 7.9 mA/cm^2. For PCDTBT, the theoretical short-circuit current density obtained from the EQE versus $PC_{71}BM$ (1:4 ratio) curve was 6.6 mA/cm^2. The EQE of PC-TBT-TQ is higher than that of PCDTBT due to the higher molecular weight of PC-TBT-TQ (216.2 kg/mol) compared to that of PCDTBT (18.4 kg/mol).

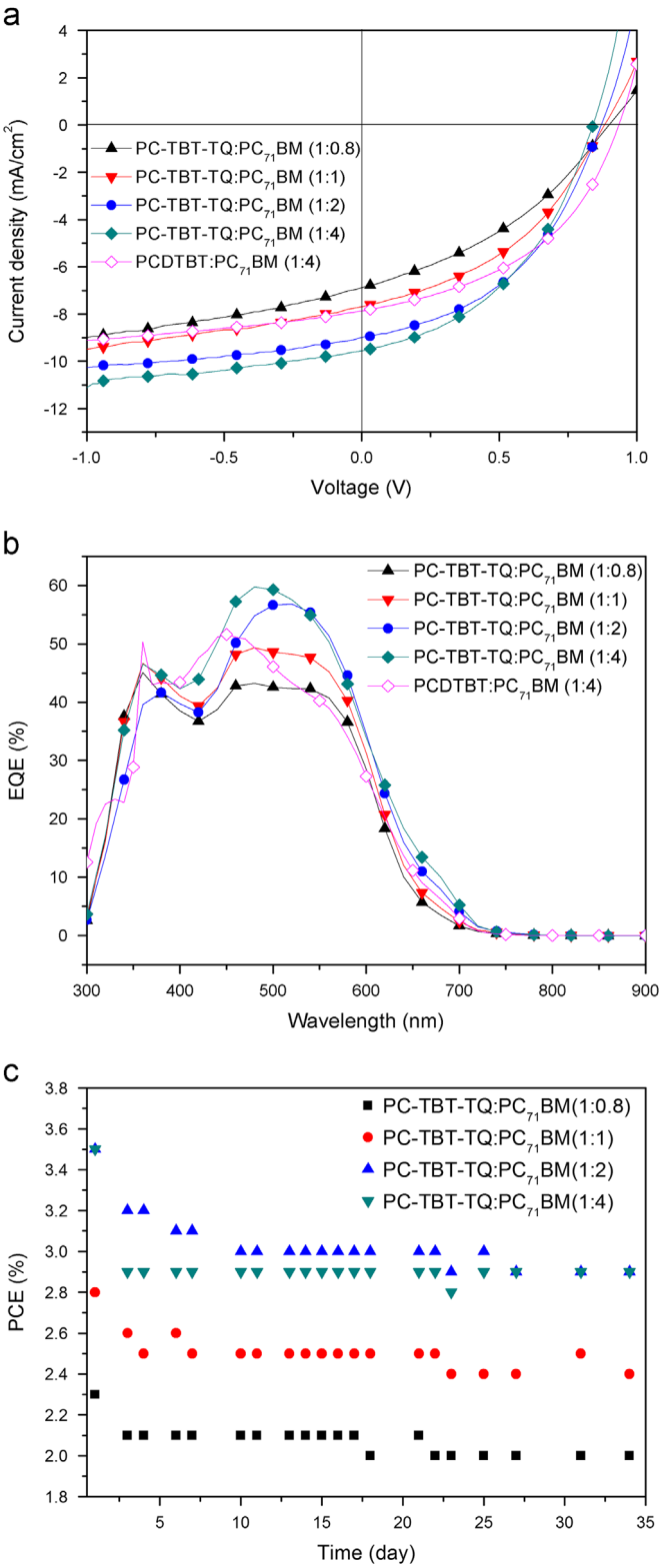

Fig. 6. (a) *J*–*V* characteristics and (b) EQE spectra of BHJ solar cells; (c) durability test data of photovoltaic devices based on PC-TBT-TQ as donor material

To investigate the oxidative stability of photovoltaic devices based on PC-TBT-TQ, the current density–voltage (*J*–*V*) curves of the devices were measured under ambient conditions for a month. All of the devices were encapsulated to prevent oxidation of

the metal electrode and were placed under ambient conditions. As shown in Fig. 6(c), the PCE values of the devices based on PC-TBT-TQ as a donor material changed little after 2 days. Moreover, the PCE values of these devices decreased by only approximately 20% even after a month, which was supposed to originate from the electrochemical stability of the donor polymers, as mentioned above [28].

Table 3
Photovoltaic performance of the BHJ solar cells.

Active layer (w/w)		Weight ratio (P:A, w/w)	V_{OC} (V)	J_{SC} (mA/cm^2)	FF (%)	PCE (%)
Polymer (P)	Acceptor (A)					
PC-TBT-TQ	$PC_{71}BM$	1:08	0.89	6.8	36.8	2.3
		1:1	0.87	7.7	41.4	2.8
		1:2	0.87	9.0	44.0	3.5
		1:4	0.83	9.5	43.3	3.5
PCDTBT	$PC_{71}BM$	1:4	0.89	7.8	47.5	3.3

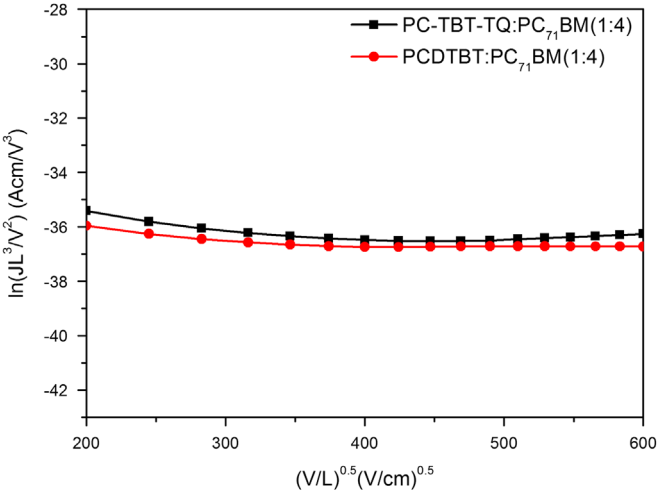

Fig. 7. *J–V* characteristics of hole-only devices

Fig. 7 shows the *J–V* characteristics of the hole-only devices based on PC-TBT-TQ:$PC_{71}BM$ and PCDTBT:$PC_{71}BM$ blends. Hole-only devices were fabricated with a diode configuration of ITO (170 nm)/PEDOT:PSS(40 nm)/polymer:$PC_{71}BM$(50 nm)/MoO_3(30 nm)/Al (100 nm). We used the space charge limited current (SCLC) model to determine the hole mobility in blends with $PC_{71}BM$. The hole mobilities of PC-TBT-TQ:$PC_{71}BM$ (1:4 ratio) and PCDTBT:$PC_{71}BM$ (1:4 ratio) were estimated to be approximately 9.03×10^{-4} cm^2 V^{-1} s^{-1} and 6.11×10^{-4} cm^2 V^{-1} s^{-1}, respectively. The hole mobility of PC-TBT-TQ was higher than that of PCDTBT due to the former's high molecular weight and face-on orientation [26,29]. The electron mobility (1.6×10^{-2} cm^2 V^{-1} s^{-1}) of $PC_{71}BM$ was close to the hole mobility of PC-TBT-TQ:$PC_{71}BM$ (1:4 ratio) than PCDTBT:$PC_{71}BM$ (1:4 ratio), resulting in an balance in the hole and electron transport in the PC-TBT-TQ:$PC_{71}BM$ (1:4 ratio) film [30,31].

3.6. Morphology analysis

To investigate the morphology of the polymer/PCBM blend film, atomic force microscopy (AFM) was performed, and the results are shown in Fig. 8.

As shown in Fig. 8(a), softened boundaries were observed in PC-TBT-TQ:$PC_{71}BM$ 1:4(3×3 μm^2), which indicate a micro-phase separation between the polymer and PCBM. Smooth micro-phase separation was more pronounced when measured over a 1×1 μm^2 area. All of the high-molecular-weight films appeared to have an isotropic nodule-like structure [32]. The migration of charge carriers was facilitated by the formation of a charge transport pathway in the ordered region by making contact with the long polymer backbones.

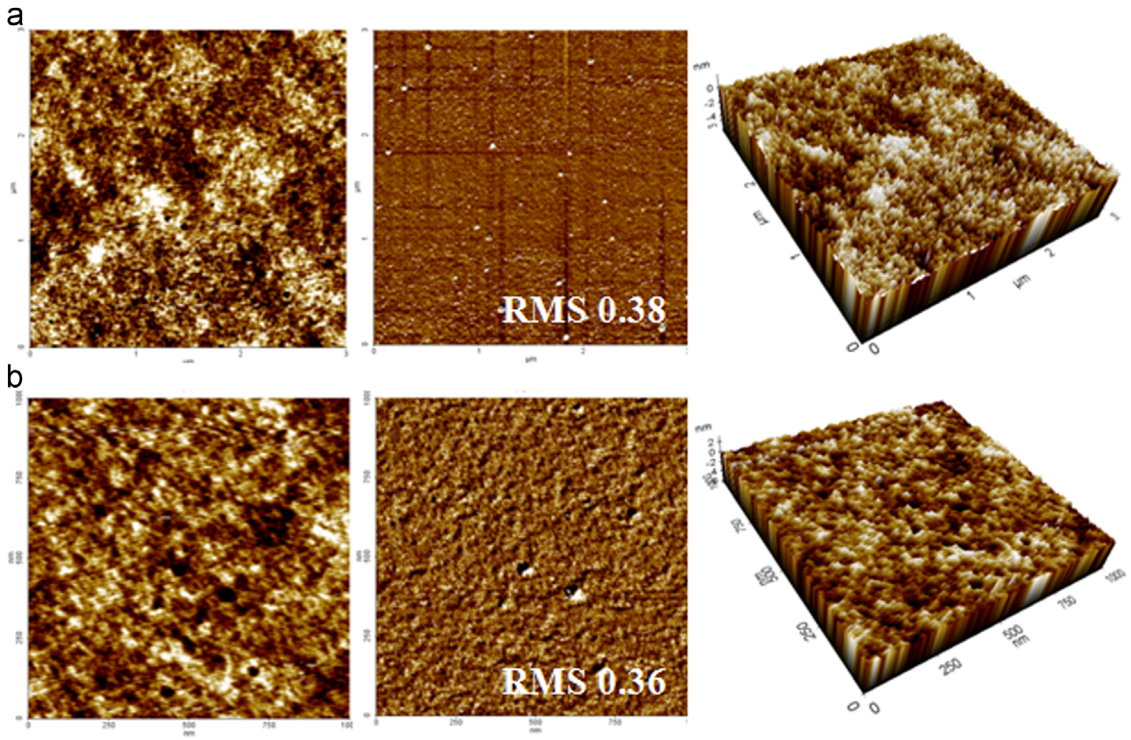

Fig. 8. Topographic AFM images of films with PC-TBT-TQ:$PC_{71}BM$ ratios of 1:4: (a) 3×3 μm^2 and 1×1 μm^2

4. Conclusions

We successfully synthesized PC-TBT-TQ through the Suzuki coupling reaction by introducing carbazole, dithienylbenzothiadiazole and dithienylquinoxaline units. PC-TBT-TQ showed a high molecular weight, thermal stability, air stability and a band gap of 1.89 eV due to the low HOMO energy level of the polymer.

PC-TBT-TQ showed greater solar absorption over the range of 500–700 nm, where photons were abundant. When the ratio of PC-TBT-TQ to $PC_{71}BM$ was 1:4, the open-circuit voltage (V_{OC}) was 0.83 V, the short-circuit current (J_{SC}) was 9.5 mA/cm^2, the fill factor (FF) was 43.3% and the power conversion efficiency (PCE) was 3.5%. It is likely that higher performance levels could be attained if the chemical structure and device structure of the polymer were optimized.

Acknowledgements

This research was supported by a grant from the Fundamental R&D Program for Core Technology of Materials funded by the Ministry of Knowledge Economy, Republic of Korea (10037195) and by the National Research Foundation of Korea Grant funded by the Korean Government (MEST) (NRF-2009-C1AAA001-2009-0093526).

References

[1] R.H. Friend, R.W. Gymer, A.B. Holmes, J.H. Burroughes, R.N. Marks, C. Taliani, D.D.C. Bradley, D.A.D. Santos, J.L. Bredas, M. Logdlund, W.R. Salaneck, Electroluminescence in conjugated polymers, Nature 397 (1999) 121–128.
[2] W. Lu, J. Kuwabara, T. Kanbara, Polycondensation of dibromofluorene analogues with tetrafluorobenzene via direct arylation, Macromolecules 44 (2011) 1252–1255.
[3] H.J. Song, J.Y. Lee, I.S. Song, D.K. Moon, J.R. Haw, Synthesis and electroluminescence properties of fluorene–anthracene based copolymers for blue and white emitting diodes, Journal of Industrial and Engineering Chemistry 17 (2011) 352–357.
[4] A. Iwan, M. Palewicz, A. Chuchmała, L. Gorecki, A. Sikora, B. Mazurek, G. Pasciak, Opto(electrical) properties of new aromatic polyazomethines with fluorene moieties in the main chain for polymeric photovoltaic devices, Synthetic Metals 162 (2012) 143–153.
[5] J.Y. Lee, S.H. Kim, I.S. Song, D.K. Moon, Efficient donor–acceptor type polymer semiconductors with well-balanced energy levels and enhanced open circuit voltage properties for use in organic photovoltaics, Journal of Materials Chemistry 21 (2011) 16480–16487.
[6] J. Zhang, W. Cai, F. Huang, E. Wang, C. Zhong, S. Liu, M. Wang, C. Duan, T. Yang, Y. Cao, Synthesis of quinoxaline-based donor – acceptor narrow-band-gap polymers and their cyclized derivatives for bulk-heterojunction polymer solar cell applications, Macromolecules 44 (2011) 894–901.
[7] F.C. Krebs, J. Fyenbo, M. Jorgensen, Product integration of compact roll-to-roll processed polymer solar cell modules: Methods and manufacture using flexographic printing, slot-die coating and rotary screen printing, Journal of Materials Chemistry 20 (2010) 8994–9001.
[8] Y. Dong, W. Cai, X. Hu, C. Zhong, F. Huang, Y. Cao, Synthesis of novel narrow-band-gap copolymers based on [1,2,5]thiadiazolo[3,4-f]benzotriazole and their application in bulk-heterojunction photovoltaic devices, Polymer 53 (2012) 1465–1472.
[9] M. Manceau, D. Angmo, M. Jørgensen, F.C. Krebs, Ito-free flexible polymer solar cells: from small model devices to roll-to-roll processed large modules, Organic Electronics 12 (2011) 566–574.
[10] F.C. Krebs, Polymer solar cell modules prepared using roll-to-roll methods: knife-over-edge coating, slot-die coating and screen printing, Solar Energy Materials and Solar Cells 93 (2009) 465–475.
[11] T. Yamamoto, H. Kokubo, M. Kobashi, Y. Sakai, Alignment and field-effect transistor behavior of an alternative π-conjugated copolymer of thiophene and 4-alkylthiazole, Chemistry of Materials 16 (2004) 4616–4618.
[12] T. Yasuda, Y. Sakai, S. Aramaki, T. Yamamoto, New coplanar (aba)n-type donor – acceptor π-conjugated copolymers constituted of alkylthiophene (unit a) and pyridazine (unit b): synthesis using hexamethylditin, self-organized solid structure, and optical and electrochemical properties of the copolymers, Chemistry Materials 17 (2005) 6060–6068.
[13] J.C. Bijleveld, A.P. Zoombelt, S.G.J. Mathijssen, M.M. Wienk, M. Turbiez, D.M. de Leeuw, R.A.J. Janssen, Poly(diketopyrrolopyrrole – terthiophene) for ambipolar logic and photovoltaics, Journal of the American Chemical Society 131 (2009) 16616–16617.
[14] H.-C. Chen, Y.-H. Chen, C.-C. Liu, Y.-C. Chien, S.-W. Chou, P.-T. Chou, Prominent short-circuit currents of fluorinated quinoxaline-based copolymer solar cells with a power conversion efficiency of 8.0%, Chemistry of Materials 24 (2012) 4766–4772.
[15] J.Y. Lee, W.S. Shin, J.R. Haw, D.K. Moon, Low band-gap polymers based on quinoxaline derivatives and fused thiophene as donor materials for high efficiency bulk-heterojunction photovoltaic cells, Journal of Materials Chemistry 19 (2009) 4938–4945.
[16] A.V. Patil, W.-H. Lee, E. Lee, K. Kim, I.-N. Kang, S.-H. Lee, Synthesis and photovoltaic properties of a low-band-gap copolymer of dithieno[3,2-b:2′,3′-d]thiophene and dithienylquinoxaline, Macromolecules 44 (2011) 1238–1241.
[17] N. Blouin, A. Michaud, D. Gendron, S. Wakim, E. Blair, R. Neagu-Plesu, M. Belletête, G. Durocher, Y. Tao, M. Leclerc, Toward a rational design of poly (2,7-carbazole) derivatives for solar cells, Journal of the American Chemical Society 130 (2007) 732–742.
[18] Y. Lee, Y.M. Nam, W.H. Jo, Enhanced device performance of polymer solar cells by planarization of quinoxaline derivative in a low-bandgap polymer, Journal of Materials Chemistry 21 (2011) 8583–8590.
[19] H.-J. Song, D.-H. Kim, E.-J. Lee, S.-W. Heo, J.-Y. Lee, D.-K. Moon, Conjugated polymer consisting of quinacridone and benzothiadiazole as donor materials for organic photovoltaics: coplanar property of polymer backbone, Macromolecules 45 (2012) 7815–7822.
[20] H.J. Song, S.M. Lee, J.Y. Lee, B.H. Choi, D.K. Moon, The synthesis and electroluminescent properties of dithienylquinacridone-based copolymers for white light-emitting diodes, Synthetic Metals 161 (2011) 2451–2459.
[21] F.M. Pasker, M.F.G. Klein, M. Sanyal, E. Barrena, U. Lemmer, A. Colsmann, S. Höger, Photovoltaic response to structural modifications on a series of conjugated polymers based on 2-aryl-2h-benzotriazoles, Journal of Polymer Science Part A: Polymer Chemistry 49 (2011) 5001–5011.
[22] Y. Zhu, R.D. Champion, S.A. Jenekhe, Conjugated donor – acceptor copolymer semiconductors with large intramolecular charge transfer: synthesis, optical properties, electrochemistry, and field effect carrier mobility of thienopyrazine-based copolymers, Macromolecules 39 (2006) 8712–8719.
[23] J. Hou, T.L. Chen, S. Zhang, L. Huo, S. Sista, Y. Yang, An easy and effective method to modulate molecular energy level of poly(3-alkylthiophene) for high-voc polymer solar cells, Macromolecules 42 (2009) 9217–9219.
[24] J.-M. Jiang, P.-A. Yang, T.-H. Hsieh, K.-H. Wei, Crystalline low-band gap polymers comprising thiophene and 2,1,3-benzooxadiazole units for bulk heterojunction solar cells, Macromolecules 44 (2011) 9155–9163.
[25] G. Lu, H. Usta, C. Risko, L. Wang, A. Facchetti, M.A. Ratner, T.J. Marks, Synthesis, characterization, and transistor response of semiconducting silole polymers with substantial hole mobility and air stability. Experiment and theory, Journal of the American Chemical Society 130 (2008) 7670–7685.
[26] S. Subramaniyan, H. Xin, F.S. Kim, S. Shoaee, J.R. Durrant, S.A. Jenekhe, Effects of side chains on thiazolothiazole-based copolymer semiconductors for high performance solar cells, Advanced Energy Materials 1 (2011) 854–860.
[27] A. Gadisa, W. Mammo, L.M. Andersson, S. Admassie, F. Zhang, M.R. Andersson, O. Inganäs, A new donor–acceptor–donor polyfluorene copolymer with balanced electron and hole mobility, Advanced Functional Materials 17 (2007) 3836–3842.
[28] M.O. Reese, S.A. Gevorgyan, M. Jørgensen, E. Bundgaard, S.R. Kurtz, D.S. Ginley, D.C. Olson, M.T. Lloyd, P. Morvillo, E.A. Katz, A. Elschner, O. Haillant, T.R. Currier, V. Shrotriya, M. Hermenau, M. Riede, K.R. Kirov, G. Trimmel, T. Rath, O. Inganäs, F. Zhang, M. Andersson, K. Tvingstedt, M. Lira-Cantu, D. Laird, C. McGuiness, S. Gowrisanker, M. Pannone, M. Xiao, J. Hauch, R. Steim, D.M. De Longchamp, R. Rösch, H. Hoppe, N. Espinosa, A. Urbina, G. Yaman-Uzunoglu, J.-B. Bonekamp, A.J.J.M. van Breemen, C. Girotto, E. Voroshazi, F.C. Krebs, Consensus stability testing protocols for organic photovoltaic materials and devices, Solar Energy Materials and Solar Cells 95 (2011) 1253–1267.
[29] H.-J. Song, D.-H. Kim, E.-J. Lee, D.-K. Moon, Conjugated polymers consisting of quinacridone and quinoxaline as donor materials for organic photovoltaics: orientation and charge transfer properties of polymers formed by phenyl structures with a quinoxaline derivative, Journal of Materials Chemistry A 1 (2013) 6010–6020.
[30] A.K.K. Kyaw, D.H. Wang, H.-R. Tseng, J. Zhang, G.C. Bazan, A.J. Heeger, Electron and hole mobility in solution-processed small molecule-fullerene blend: dependence on the fullerene content, Applied Physics Letters 102 (2013) 163308.
[31] S. Wen, J. Pei, P. Li, Y. Zhou, W. Cheng, Q. Dong, Z. Li, W. Tian, Synthesis and photovoltaic properties of low-bandgap 4,7-dithien-2-yl-2,1,3-benzothiadiazole-based poly(heteroarylenevinylene)s, Journal of Polymer Science Part A: Polymer Chemistry 49 (2011) 2715–2724.
[32] R.J. Kline, M.D. McGehee, E.N. Kadnikova, J. Liu, J.M.J. Fréchet, M.F. Toney, Dependence of regioregular poly(3-hexylthiophene) film morphology and field-effect mobility on molecular weight, Macromolecules 38 (2005) 3312–3319.